An Oblique Incidence Ion Implanted MSFVW RAF with Linear Group Delay

G-20

K.W. Reed, J.M. Owens, R.L. Carter, and C.V. Smith
Electronic Materials and Device Engineering Research Laboratory
The University of Texas at Arlington, 76019

ABSTRACT

Ion implanted bars have been used in a MSFVW oblique incidence reflective array linear delay filter at 3 GHz. Theory and synthesis techniques are presented based on a four layer complex dispersion relation and the impulse reflection model.

INTRODUCTION

Magnetostatic Wave (MSW) devices have been developed with signal processing capabilities analogous to SAW [1], but in the 1-20 GHz range with bandwidths approaching 2 GHz. MSW'S are slow, dispersive, magnetically dominated waves, which propagate in magnetically biased ferrite materials. High quality, low loss Yttrium Iron Garnet (YIG) films grown on Gadolinium Gallium Garnet substrates by liquid phase epitaxy (LPE) are routinely achieved with propagation losses of less than 13 dB/μsec.

Numerous significant MSW devices have been reported which perform microwave signal processing functions, including normal [2,3], and oblique incidence [4,5] reflective array filters (RAF's). Initial studies [6,7] of periodic reflecting structures have shown that periodic etched grooves and metal bar or dot arrays can provide periodic impedance variations in the EPI-YIG, yielding filter action. Metal arrays tend to exhibit high losses in the metalized YIG region. Etched grooves used with magnetostatic forward volume waves (MSFVW) in oblique incidence RAF's suffer fringe field coupling to vertical spin modes at the sharp groove edges [8]. Ion implanted bars in this same context have been shown to be free of spin mode conversion at the effectively smoother implant interface and give good agreement with a simple theory.

This paper presents theoretical modeling and experimental results on the performance of a Boron ion implanted, nonuniform oblique incidence MSFVW RAF exhibiting a nominally linear group delay characteristic over a 300 MHz bandwidth centered at 3.2 GHz. Synthesis procedures used to design the resultant transmission spectral amplitude and group delay are outlined.

THEORY

Dispersion Relation

The MSFVW bias field configuration was chosen to obtain isotropic propagation and to allow oblique reflection without requiring a mode conversion. A Polder tensor [9] was derived, assuming the thin ferrite film to be saturated along the normally directed bias field and modeling the MSW propagation as a TE mode that is uniform across the electrically narrow aperture.

A four layer structure with adjacent implanted and unimplanted ferrite layers sandwiched by two dielectric layers was used to model the implanted bar regions. A complex MSW dispersion relation was obtained from the magnetic boundry condition equations. Setting the saturation magnetization in both the ferrite regions to the unimplanted value gave the dispersion relation for the three layer land structure which is cascaded with the four layer sections in the modeling. Gilbert form for loss was included.

Wave Impedance

A characteristic wave impedance that accounts for reflection at land-bar interfaces due to transverse field discontinuities was calculated for MSFVW in terms of frequency, f, and the complex dispersion constant, k, using Faraday's law,

$$Z = \pm \frac{2\pi f \mu_o}{k}, \qquad (1)$$

assuming harmonic time variation, negligible field variation with z, y variation of the form exp±[-jky], and equating the resulting x-components. Land and bar sections were cascaded together in the theory, neglecting the effects of longitudinal field mismatch, since the thickness of the implanted reflectors was less than 2% of the total thickness of the ferrite film.

Ion Implantation Effects

Ion implantation causes a change in the characteristic wave impedance by straining the crystal lattice and reducing the saturation magnetization. The implantation doses and energies used in this work were scaled from those published by McNeal and Speriosu [10] for a double staggered implant with a roughly uniform magnetization profile in the implanted region to a depth of 0.4 μm. Doses were chosen to yield a 50% reduction in the antisotrophy field obtaining theoretical MSFVW reflectivities of 0.006, constant over the passband.

Signal Model

Reflection coefficients for the land-bar interfaces were calculated using the dispersion relations for the implanted and unimplanted regions and the characteristic impedance relation. The small constant edge reflectivities predicted by this theory justified the use of an impulse model for signal flow through the array. Beam refraction at land-bar boundries, transmission effects of leading bars, and interbar

0149-645X/83/0000-0187 $01.00 © 1983 IEEE

illumination were neglected, approximating the output signal as the sum of independent reflector contributions. Reflections from the leading and trailing edges were incorporated into the reflection coefficient for each bar. Use of an electrically short input transducer (aperture much narrower than wavelength in transducer) gave a uniform wavefront across the signal aperture. Thus, neglecting beam spreading, the power sampling of a reflector was determined as its projection onto the input transducer. Summing over N bars gives the array transfer function,

$$A(f)=j2r(f)e^{-jkz_o}\sum_{i}^{N}\sqrt{l_i/l_t}\;e^{-jky}\sin(kw_i/2) \quad (2)$$

where z_o is the distance from the array axis to the output transducer, y_i is the distance from the input transducer to the center of the ith bar, l_i/l_t is the projection of the ith bar onto the input transducer, w_i is the width of the ith bar, and $r(f)$ is the reflectivity of a land-bar interface. The transcucers were modeled as low loss shorted microstrips with MSW excitation corresponding to a radiation resistance after Wu [11]. Transducer contributions were multiplied with the array transfer function to obtain the over all filter response.

Synthesis Technique

Synthesis of the linear group delay characteristic was based on a plane wave representation of the MSFVW and the real part of the propagation constant, giving a simple relation between time delay, t, and bar position, y, with frequency, f, as a parameter,

$$t(f,y) = \frac{1}{2\pi}\frac{dRe(\mathbf{k})}{df}\,y = m(f-f_o) + t(f_o), \quad (3)$$

Inspection of the impulse model shows that peak reflection occurs when the bar width obeys

$$w = \frac{\pi}{Re[\mathbf{k}(f)]} . \quad (4)$$

Eliminating frequency from these two equations gives an implicit relation between y and w. which is iterated until the change in y from its value at the leading edge of the land or bar equals w/2, corresponding to the land or bar center. Since, each reflector responds to a different wave length (hence frequency) as determined by its width, spectral amplitude shaping is achievable by scaling each reflector length according to the desired power spectrum at the frequency it reflects. Additional reflector length weighting must be superimposed on this desired response to compensate for propagation losses exp[-Im(**k**y)] down the array and transducer spectral variations as calculated by the microstrip radiation resistance model.

EXPERIMENT

Experimental Devices

A 19 mm long, uniform 3 mm transverse aperture, 61-bar, 90° reflection transversal filter was constructed by selectively implanting a 24 μm thick YIG film with boron ions (figure 1).

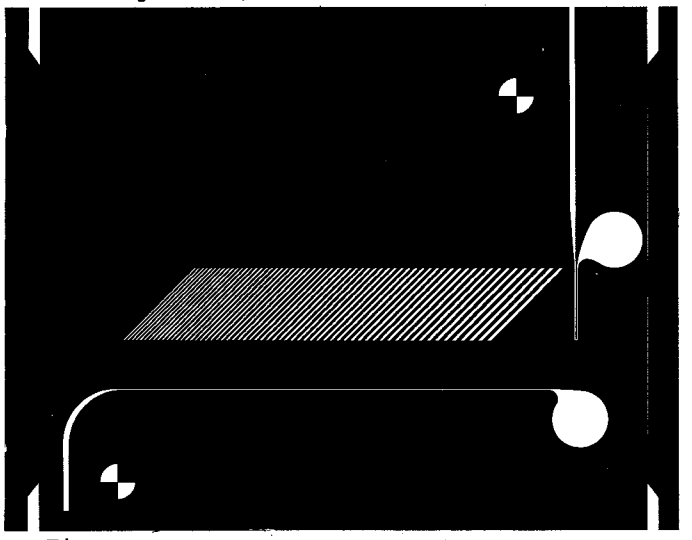

Figure 1. Mask layout showing array and transducers (3x scale).

A double dose implant (dose#1: 5.56x10^{14} cm^{-2} @ 70KeV, dose#2: 1.46x10^{15} cm^{-2} @ 200 KeV) was used producing a projected uniform step reduction in saturation magnetization of 50% to a depth of 0.4 μm. The implanted reflectors varied from 0.082 mm to 0.192 mm in width along the propagation direction giving the maximum bandwidth possible with unsectioned bars without harmonic overlap. The film was grown by liquid phase epitaxy on a 250 μm gadolinium gallium garnet substrate using a Tolksdorf melt.

Flipped configuration was used with transducers of 4 μm thick sputtered aluminum on 250 μm thick alumina substrates. A loop input transducer was used to suppress the low frequency uniform spin mode, with a 50 μm wide, 100 μm centre spaced, 3 mm aperture filament. The output transducer was a single 19 mm long 50 μm wide shorted bar.

Experiment versus Theory

Theoretical and experimental S_{21} amplitude and group delay results are compared in figure 2 on identical scales and quantitatively summarized with the design goal in table 1.

Table 1: Quantitative comparison of results.

	DELAY			INSERTION LOSS (dB)		TIME BANDWIDTH PRODUCT
	Slope (nsec/GHz)	@ 3.2 GHz (nsec)	rms DEV. from LIN. (nsec)	@ 3.1 GHz (dB)	@ 3.2 GHz (dB)	
DESIGN	600.0	120	----	free	free	free
THEORY	590.0	120	5.69	40	47	77.4
EXPERIMENT	605.7	100	8.22	33	47	77

The experimental insertion loss shows a peaking at the lower frequencies that is not predicted by the theory. This effect is attributed to the frequency response of the electrically long output transducer (l = 19 mm and λ(3GHz) = 3 cm) which was modeled as electrically short in the theory.

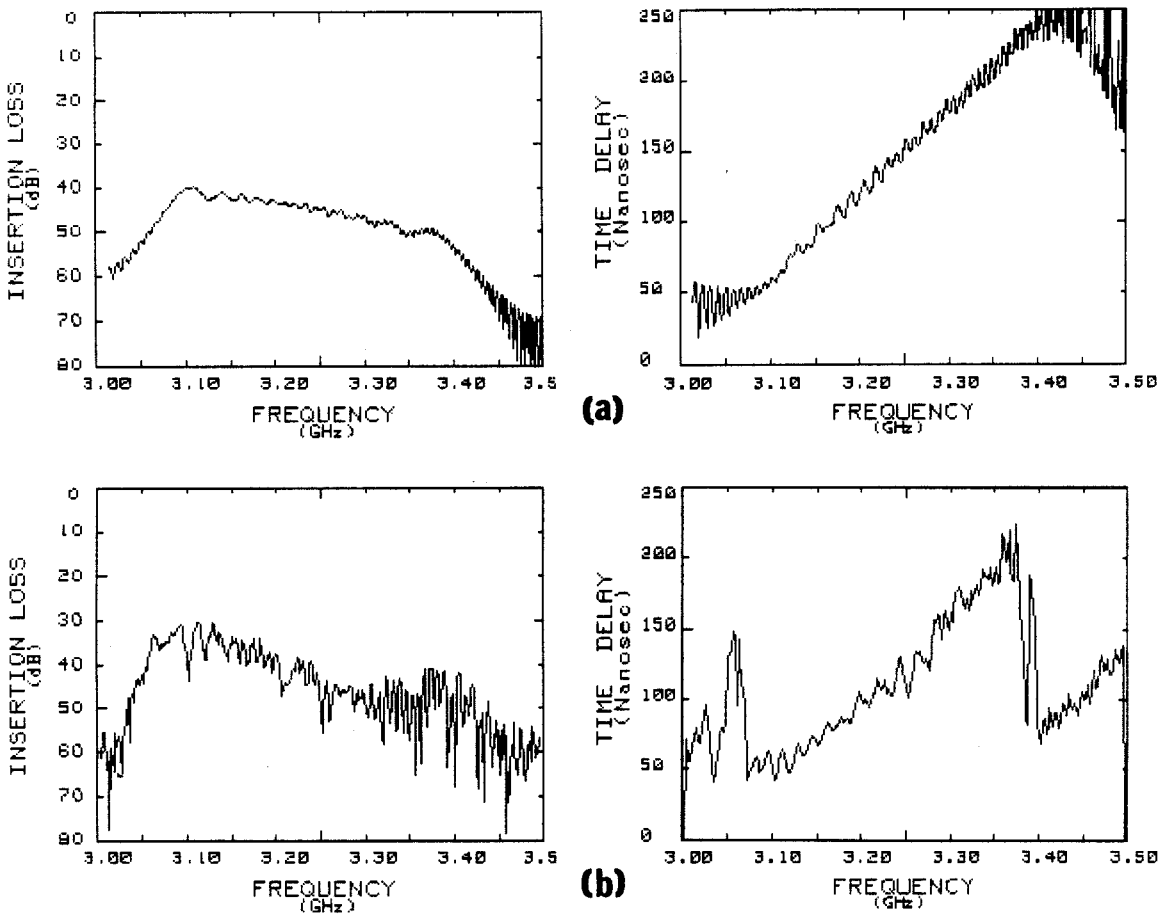

Figure 2. (a) theoretical transmission insertion loss and group delay. (b) experimental transmission insertion loss and group delay.

Use of a lower permitivity substrate material such as quartz should eliminate this problem. A greater rms deviation from linear is expected in the experimental results with the effects of edge reflections added to the Fresnel ripple anticipated by theory. Sandblasting was used on the crystal edges to reduce reflections, but angle lapping or pole face end beveling may have provided better results. Delay slopes and intercepts for theory and experiment are in good agreement allowing for uncertainties in array alignment and film thickness, both of which could add curvature or absolute delay to the overall response. The second array harmonic can be seen in the experimental result beginning 300 MHz above the low frequency edge of the fundamental. The presence of this second harmonic is corroborated by the corresponding sudden retrace in the experimental group delay response. To reduce this harmonic, bar sectioning will be tested in the future.

ACKNOWLEDGEMENTS

The Air Force Office of Scientific Research is acknowledged for support of this work through grant AFOSR 80-0264. The authors extend special thanks to Texas Instruments for performing the implants.

REFERENCES

1. J. M. Owens, R. L. Carter, C. V. Smith, and J. H. Collins, 1980 Ultrasonics Symposium Proceedings, p. 506, IEEE #80CH1602-2.

2. J.M.Owens, C. V. Smith, Jr., E. P. Snapka and J. H. Collins, 1978 IEEE International Microwave Symposium, p. 440, Cat.78CH1355-7

3. R. L. Carter, J. M. Owens, C. V. Smith, Jr. and K. W. Reed, J. Appl. Phys. 53(3), March 1982, p. 2655.

4. G. Volluet and P. Hartemann, 1981 Ultrasonics Symposium Proceedings, Vol. 1 p. 394, Cat. 81CH1689-9.

5. R. L. Carter, J. M. Owens, C. V. Smith, and K. W. Reed, 1982 IEEE International Microwave Symposium, p. 83, Cat.82CH1705-3.

6. C. G. Sykes, J. D. Adams and J. H. Collins Appl. Phys. Lett. 29, 388, (1976).

7. J. M. Owens, et al, IEEE Trans. Mag. 14 388 (1976).

8. R. L. Carter, C. V. Smith, Jr., and J. M. Owens, IEEE Trans. Mag. 16,1159 (1980).

9. D. Polder, Phil. Mag. 40, p. 99 (1949).

10. B. E. MacNeal and V. S. Speriosu, J. Appl. Phys. 52, p.3935 (1981).

11. HJ. Wu, Ph.D. Dissertation, The University of Texas at Arlington, Arlington Texas (1978).